Influence of wave phase difference between surface soil heat flux and soil surface temperature on land surface energy balance closure

Z. GAO[1], R. HORTON[2], H. P. LIU[3], J. Wen[4], L. Wang[1]

1. *State Key Laboratory of Atmospheric Boundary Layer Physics and Atmospheric Chemistry, Institute of Atmospheric Physics, CAS, Beijing, China*
2. *Department of Agronomy, Iowa State University, Ames, Iowa, USA*
3. *Department of Physics, Atmospheric Sciences, and Geosciences, Jackson State University, Jackson, Mississippi, USA*
4. *Cold and Arid Regions Environmental and Engineering Research Institute, CAS, Lanzhou, China*

Abstract

The sensitivity of climate simulations to the diurnal variation in surface energy budget encourages enhanced inspection into the energy balance closure failure encountered in micrometeorological experiments. The diurnal wave phases of soil surface heat flux and temperature are theoretically characterized and compared for both moist soil and absolute dry soil surfaces, indicating that the diurnal wave phase difference between soil surface heat flux and temperature ranges from 0 to $\pi/4$ for natural soils. Assuming net radiation and turbulent heat fluxes have identical phase with soil surface temperature, we evaluate potential contributions of the wave phase difference on the surface energy balance closure. Results show that the sum of sensible heat flux (H) and latent heat flux (LE) is always less than surface available energy ($Rn-G_0$) even if all energy components are accurately measured, their footprints are strictly matched, and all corrections are made. The energy balance closure ratio (ε) is extremely sensitive to the ratio of soil surface heat flux amplitude (A_4) to net radiation flux amplitude (A_1), and

large value of A_4 / A_1 causes a significant failure in surface energy balance closure. An experimental case study confirms the theoretical analysis.

1. Introduction

The energy balance equation is widely applied to examine ground and canopy surface temperatures in land surface models which are usually coupled in mesoscale and climate models (e.g., Sellers *et al*., 1996; Chen and Dudhia, 2001; and Gao *et al*., 2004). The land surface energy balance equation includes the following major components of the surface energy budget: net radiation Rn (in both the visible and infrared part of the spectrum), sensible heat flux H (exchange of heat between the surface and the atmosphere by conduction and convection), latent heat flux LE (evaporation of water from the surface, where L is the latent heat of vaporization, and E is the vaporization), and heating G_0 of materials on the surface (soil, plants, water, etc.) with a small fraction converted to chemical energy when plants are present. i.e.,

$$Rn - G_0 = H + LE . \quad (1)$$

Unfortunately, from early measurements (Elagina *et al*., 1973, 1978), the First International Satellite Land Surface Climatology Project (ISLSCP) Field Experiment (FIFE) (Kanemasu *et al*., 1992), to the network of eddy covariance sites measuring long-term carbon and energy fluxes (FLUXNET) (Wilson, *et al*., 2002) and a recent energy balance experiment (EBEX-2000) (Oncley *et al*., 2007), surface energy imbalance has been observed. Foken *et al*. (1999) pointed out that the causes of the imbalance in the energy budget were usually related to the errors in the individual energy component measurements and the influence of different footprints on the individual energy components. Wilson *et al*. (2002) evaluated the energy balance closure across 22 sites and 50 site-years in FLUXNET by statistical regression of turbulent energy fluxes (sensible and latent heat (LE)) against available energy (net radiation, less the energy stored) and by solving for the energy balance ratio, the ratio of turbulent energy fluxes to available energy. Their methods indicate a general lack of closure at most sites, with a mean imbalance of about 20%. The imbalance was prevalent in all measured vegetation types and in climates ranging from Mediterranean to temperate and arctic. Foken *et al*.(2006) examined the influence of the low frequency part of the turbulence spectrum on the residual energy observed, and found that the eddy-covariance method underestimates turbulent fluxes for measuring times longer than the typical averaging interval of 30 min. Oncley *et al*. (2007) characterized the imbalance results obtained in the EBEX-2000, a study examining the ability of state-of-the-art measurements to close the surface energy balance for a flood-irrigated cotton field on uniform terrain. They concluded that (1) the EBEX dataset still indicated an energy imbalance on the order of 10% (the signed diurnal average), despite critical attention to calibration, maintenance, and software corrections of data for all sensors; and (2) the nighttime energy budget closure was good, so most of the observed imbalance was during the day. The imbalance quickly grows to nearly its midday value, suggesting that the cause does not simply scale with any one of the energy balance terms. Jacobs *et al*. (2007) examined the surface energy budget over a mid-latitude grassland in central Netherlands by taking account of all possible enthalpy changes and by correcting soil surface heat flux, resulting in a closure of 96%, which demonstrated that the correction to soil surface heat flux was important to obtain surface energy balance closure. Cava *et el*.(2008) investigated the short-term closure of the surface energy budget by using two datasets of measurements of surface heat fluxes taken at a Mediterranean site in southern Italy in the spring (2005) and autumn (2006). Their analysis showed that (1) correction of the wind speed measurement sonic anemometer error at large measurement angles has influence on the energy budget closure; and (2) an important contribution also comes from heat storage between the soil flux sensor and the ground surface, not only for the amplitude but also for the relative phases of the measured fluxes. Foken (2008) overviewed the latest 20 years work on the energy balance closure problem, and found that the exchange processes on larger scales of the heterogeneous landscape have a significant influence on surface energy balance. Su *et al*. (2008) examined the energy closure for both 10-min and 60-min averaged fluxes collected in the intensive field campaigns carried out at the Barrax agricultural test site in Spain during 12-21 July 2004 (SPARC 2004), and found that the energy closure is not reached, with the sum of the turbulent fluxes ($H+LE$) measured by the eddy covariance system being 10% higher than the available energy ($Rn-G_0$).

Soil surface heat flux (G_0) was determined by summing the heat flux at a reference depth (z) few centimeters below the surface and the rate of change of heat storage in the soil above z. Ochsner *et al*. (2006) experimentally demonstrated that heat flux plates underestimated soil heat flux, Sauer *et al*. (2006) investigated the impact of heat flow distortion and thermal contact resistance on soil heat flux plates, and Ochsner *et al*. (2007) further investigated how choices regarding z, soil volumetric heat capacity measurements, and heat storage calculations all affect the accuracy of heat storage.

Persistent concerns regarding surface energy balance closure encourage increased scrutiny of potential sources of errors (Sauer *et al*., 2006). However, can the surface energy components achieve balance closure for ideal conditions when (1) they are accurately measured, (2) their footprints are strictly matched, and (3) all corrections are made? To answer this question, the objective of present work is to characterize the phase difference between soil surface heat flux and temperature and to investigate whether it influences land surface energy balance closure by using theoretical analysis and experimental evaluation.

1. Theoretic analysis

2.1 Phase difference between soil surface heat flux and soil surface temperature

(1). Moist soil surfaces

Gao *et al*. (2003) considered soil thermal conduction and convection as follows,

$$\frac{\partial T}{\partial t} = k\frac{\partial^2 T}{\partial z^2} + W\frac{\partial T}{\partial z}, \tag{2}$$

where T is the soil temperature at a reference depth z (the vertical coordinate positive downward), t is time, k is the soil thermal diffusivity, $W \equiv \frac{\partial k}{\partial z} - \frac{C_W}{C_g} w\varphi$ where C_g is the volumetric heat capacity of soil, C_W is the volumetric heat capacity of water, w is the liquid water flux (m^3 s^{-1} m^{-2}) (positive downward), and φ is the volumetric water content of the soil. Assuming semi-infinite space with surface temperature boundary condition:

$$T(0,t) = T_1 + A\sin\omega t, \quad (t \ge 0), \tag{3}$$

where T_1 is the mean soil surface temperature, A is the amplitude of the diurnal soil surface temperature wave, and ω is the angular velocity of the Earth's rotation and $\omega = 2\pi/(24\times 3600)$ rad s^{-1}, the solution to Equation (2) is

$$\begin{aligned} T(z,t) = T_1 + A\exp&\left[(-\frac{W}{2k} - \frac{\sqrt{2}}{4k}\sqrt{W^2+\sqrt{W^4+16k^2\omega^2}})z\right] \\ &\cdot\sin\left[\omega t - z\frac{\sqrt{2}\omega}{\sqrt{W^2+\sqrt{W^4+16k^2\omega^2}}}\right] \end{aligned} \tag{4a}$$

Letting $M = 1/(\frac{W}{2k} + \frac{\sqrt{2}}{4k}\sqrt{W^2+\sqrt{W^4+16k^2\omega^2}})$ and $N = \frac{\sqrt{W^2+\sqrt{W^4+16k^2\omega^2}}}{\sqrt{2}\omega}$,

Equation (4a) becomes

$$T(z,t) = T_1 + A\exp(-z/M)\sin(\omega t - z/N)\,. \tag{4b}$$

Based on Van Wijk and De Vries (1963), the subsurface heat flux $G(z,t)$ at depth z may be written,

$$G(z,t) = -\lambda \partial T / \partial z\,, \tag{5a}$$

where λ is the thermal conductivity. Substituting Equation (4b) into Equation (5a) yields

$$\begin{aligned} G(z,t) &= \frac{\lambda A}{M}\exp(-z/M)\sin(\omega t - z/N) + \frac{\lambda A}{N}\exp(-z/M)\cos(\omega t - z/N) \\ &= \lambda A\exp(-z/M)[\frac{1}{M}\sin(\omega t - z/N) + \frac{1}{N}\cos(\omega t - z/N)] \\ &= \lambda A\exp(-z/M)\frac{\sqrt{M^2+N^2}}{MN}\sin(\omega t - z/N + \delta) \end{aligned} \tag{5b}$$

where we define $\sin\delta = \dfrac{M}{\sqrt{M^2+N^2}}$ and $\cos\delta = \dfrac{N}{\sqrt{M^2+N^2}}$. Comparing Equation (5b) against Equation (4b) shows that the wave phase difference between soil heat flux $G(z,t)$ and soil temperature $T(z,t)$ is δ rad and that $G(z,t)$ reaches its peak earlier than $T(z,t)$.

In micrometeorological experiments, soil heat flux $G(z,t)$ is directly measured by soil heat flux plates at a depth z, and the soil surface heat flux $G(0,t)$ (which is same as G_0 in Equation (1)) is then calculated by

$$G(0,t) = G(z,t) + C_g z \partial T_g / \partial t\,, \tag{6}$$

where $C_g z \partial T_g / \partial t$ is the soil heat storage in the soil layer immediately above the heat flux plates, and T_g is the vertically averaged soil temperature of this soil layer, which is usually measured by using soil temperature probes. Bruin and Holtslag (1982) applied ingenious ways to estimate $C_g z\partial T_g / \partial t$.

Theoretically,

$$T_g \equiv [T(0,t) + T(z,t)]/2. \tag{7}$$

Substituting Equations (5b) and (7) in Equation (6) yields

$$G(0,t) = \lambda A \frac{\sqrt{M^2 + N^2}}{MN} \sin(\omega t + \delta). \tag{8a}$$

Comparison of Equation (8) against Equation (3) indicates that there is a phase difference between $G(0,t)$ and $T(0,t)$ (i.e., δ, rad), and $G(0,t)$ reaches its peak $12\delta/\pi$ hours prior to $T(0,t)$. For example, when surface temperature $T(0,t)$ reaches its maximum value at 12:00 (local time), the corresponding $G(0,t)$ is probably at around 10:00 (local time) rather then at 12:00 (local time).

(2). Dry soil surfaces

Under the circumstance with homogeneous soils in which it is assumed that soil thermal diffusivity is vertically homogeneous (i.e., $\frac{\partial k}{\partial z} = 0$) and liquid water flux is negligible (i.e., $w = 0$), we obtain $W \equiv \frac{\partial k}{\partial z} - \frac{C_W}{C_g} w\varphi = 0$, therefore $N = M = d \equiv \sqrt{2k/\omega}$, and thus Equations (4b) becomes

$$T(z,t) = T_1 + A\exp(-z/d)\sin(\omega t - z/d), \tag{4c}$$

Equations (5b) becomes

$$\begin{aligned} G(z,t) &= \frac{\lambda A}{d}\exp(-z/d)\left[\sin(\omega t - z/d) + \cos(\omega t - z/d)\right] \\ &= \frac{\sqrt{2}\lambda A}{d}\exp(-z/d)\sin(\omega t - z/d + \frac{\pi}{4}) \end{aligned}, \qquad (5c)$$

and Equation (8) becomes

$$G(0,t) = \frac{\sqrt{2}\lambda A}{d}\sin(\omega t + \frac{\pi}{4}) . \qquad (8b)$$

We expect $W = 0$ for homogeneous soil experiencing conduction-only heat transfer, such as dry hot lake beds or deserts. Comparison of Equation (5c) against Equation (4c) shows that the phase difference between soil heat flux $G(z,t)$ and soil temperature $T(z,t)$ is $\pi/4$ (i.e., 3 hours), and $G(z,t)$ reaches its maximum values 3 hours prior to $T(z,t)$ in dry soils. Similarly, comparison of Equation (8b) against Equation (3) shows that the wave phase difference between surface soil heat flux $G(0,t)$ and surface soil temperature $T(0,t)$ in dry soils is $\pi/4$ (i.e., 3 hours), and $G(0,t)$ reaches its maximum values three hours prior to $T(0,t)$. The phase difference of $\pi/4$ between surface soil heat flux $G(0,t)$ and surface soil temperature $T(0,t)$ was also reported by Horton and Wierenga (1983). For example, when surface temperature $T(0,t)$ reaches its maximum value at 12:00 (local time) at a dry soil site, the corresponding $G(0,t)$ occurs around 09:00 (local time) rather then at 12:00 (local time). To illustrate these different variation patterns in $G(z,t)$, $T(z,t)$, $G(0,t)$, and $T(0,t)$ we respectively apply Equations (5c), (4c), and (8’) for a dry hot desert soil with typical parameters, e.g., $z = 0.05$ m, $k = 6.2\times10^{-7}$ m^2 s^{-1}, $C_g = 1.16\times10^6$ J m^{-3} K^{-1}, $A = 30$ K, and $T_1 = 291.76$ K, resulting in $d = 0.13$ m, and $\lambda = 0.72$ J m^{-1} K^{-1} s^{-1} (Gao *et al.*, 2007). Figure 1 shows the temporal variations in $T(0,t)$, $T(z,t)$, $G(0,t)$, $G(z,t)$, and

$C_g z \partial T_g / \partial t$ during daytime when the peak of $T(0,t)$ is set to occur at 1200 (Local time). It is found that (1) the peak of $G(0,t)$ occurs at 0900 am, i.e., 3 hours earlier than the peak of $T(0,t)$; (2) the soil surface heat flux might exceed 230 W m^{-2} if the diurnal amplitude (A) of soil surface temperature in Equation (3) is as large as 30 K in a dry hot desert soil; and (3) both of the peaks of $G(z,t)$ and $T(z,t)$ dampened z/d as compared with their corresponding surface peaks.

(3). Assessment of δ

It is worthy to quantify the range of δ because it has a potential impact on surface energy balance, which will be later discussed. Since $\sin\delta = \dfrac{M}{\sqrt{M^2 + N^2}}$ and $\cos\delta = \dfrac{N}{\sqrt{M^2 + N^2}}$, the magnitude of δ depends on the relative magnitudes of M and N. Both M and N depend on W, and for moist soil conditions, in response to surface soil water evaporation soil dries from the surface downward. The drying causes liquid water to move upward from the subsoil to the surface evaporation zone, and results in the soil to have a non-uniform water content vertically with depth. Due to the non-uniform water content the soil thermal diffusivity also varies with depth, and k tends to increase from the surface downward, i.e., the smallest value of k is at the dry surface and larger values of k occur in the moist subsurfaces. The direct result is that $\partial k / \partial z > 0$. As shown above, $W \equiv \dfrac{\partial k}{\partial z} - \dfrac{C_W}{C_g} w\varphi$, where w is usually expected to be only a few millimeters per day of evaporation flux. The soil water flux responds to the evaporation boundary condition so one can expect only a few millimeters per day soil water flux ($\frac{C_W}{C_g} w\varphi$), too. With this understanding, $\partial k / \partial z$ should be the main contributor to W. The fact that $\partial k / \partial z > 0$ results in $W > 0$, leading to $N > M > 0$ in the moist soils that experience evaporative drying. The fact that $N > M > 0$ directly causes $\pi / 4 > \delta > 0$.

2.2 Influence of phase difference between soil surface heat flux and soil surface temperature on surface energy balance

In this section, we characterize the potential influence of the phase difference between soil surface heat flux (G_0) and soil surface temperature ($T(z,t)$) on surface energy balance closure. Usually, micrometeorologists tabulate the time series of energy components (Rn, H, LE, and G_0), and then close them for each sample period. We assume that

$$Rn = A_1 \sin[3600\omega(t_1 - 6)],\ \ 18 \ge t_1 \ge 6; \tag{9.1}$$

$$H = A_2 \sin[3600\omega(t_1 - 6)],\ \ 18 \ge t_1 \ge 6; \tag{9.2}$$

$$LE = A_3 \sin[3600\omega(t_1 - 6)],\ \ 18 \ge t_1 \ge 6; \tag{9.3}$$

and $$G_0 = A_4 \sin[3600\omega(t_1 - 6)],\ \ 18 \ge t_1 \ge 6; \tag{9.4}$$

where t_1 is time (in hour), A_1, A_2, A_3, and A_4 are diurnal amplitudes of Rn, H, LE, and G_0, respectively. For our purpose, we assume $A_1 = 600$ W m^{-2}, $A_2 = 300$ W m^{-2}, $A_3 = 200$ W m^{-2}, and $A_4 = A_1 - (A_2 + A_3) = 100$ W m^{-2}, for an idealized land surface where the phases of all the energy components are forced to be identical to that of soil surface temperature. Figure 2 shows (a) the diurnal variations of these energy components and (b) the scatter distribution of $H+LE$ against $Rn-G_0$. It is apparent that energy balance closure occurs.

Net radiation (Rn) is usually obtained by $Rn = DSR + DLR - \mathrm{U}SR - \mathrm{U}LR$ where DSR and DLR are downward short- and long-wave radiation and $\mathrm{U}SR$ and $\mathrm{U}LR$ are upwelling reflected shortwave radiation and long-wave radiation emitted by surface, respectively. $\mathrm{U}SR = \alpha \times DSR$ where α is the surface albedo, so $\mathrm{U}SR$ and DSR have identical phase in their diurnal variations. This phase depends on the solar elevation angle. DSR is one cause of surface temperature change, and conversion of radiation to heat has a delay that depends on material properties. This delay is negligible in observation as later shown in Figure 4. Meanwhile, because $\mathrm{U}SR = \alpha \times DSR$, $\mathrm{U}SR$ has identical phase with DSR. In this way, we assume that both $\mathrm{U}SR$ and DSR have identical phase with soil surface temperature. ULR is calculated via Stefan-Boltzmann law, and has identical phase with soil surface temperature. DLR usually has identical phase with ULR. In this way, we assume that Rn has identical diurnal variation phase with the soil surface temperature.

Sensible heat flux (H) is usually obtained by using the difference of soil surface temperature and air temperature at a reference height, so we assume H has identical diurnal variation phase with soil surface temperature. Latent heat flux (LE) is usually obtained by using the difference of the specific humidity at soil surface temperature and the specific humidity at a reference height, so we assume LE has identical diurnal variation phase with soil surface temperature too. Therefore, we assume that Rn, H, and LE have identical phases with soil surface temperature although, in reality, the phases of energy components (i.e., Rn, H, and LE) may not be strictly identical to that of soil surface temperature.

The phase of soil surface heat flux G_0 differs from that of soil surface temperature, as mentioned above. For a dry soil, soil surface heat flux G_0 can be expressed as

$$G_0 = A_4 \sin[3600\omega(t_1 - 6) + \pi / 4], \text{ and } 18 \geq t_1 \geq 6. \tag{9.4'}$$

Correspondingly, the surface energy balance becomes incomplete with a closure of 92.8% only. Moreover, this result indicates that the surface energy balance closure varies during different periods of time as

$$H + LE > Rn - G_0, \qquad 10.5 > t_1 \geq 6; \tag{10.1}$$

$$H + LE = Rn - G_0, \qquad t_1 = 10.5; \tag{10.2}$$

$$\text{and } H + LE \leq Rn - G_0, \qquad 18 \geq t_1 > 10.5, \tag{10.3}$$

as shown in Figure 3a. The correlation coefficients (r) between $H + LE$ and $Rn - G_0$ is 0.96. Our theoretical analysis on Figure 3b suggests (1) that the imbalance quickly grows to nearly its midday value, which is consistent with the experimental findings in Oncley et al. (2007); and (2) that energy components in the morning should more readily achieve balance closure than those in the afternoon for the sites where soil is not absolutely dry. In Figure 3b, the green line is obtained by linear regression analysis.

We define the energy balance closure ratio $\varepsilon = (H + LE)/(Rn - G_0)$, i.e., the slope of the linear regression line which is forced to pass the origin of coordinates in Figure 3b. When Equation (9.4') holds, the energy balance closure ratio ε is extremely sensitive to the ratio of A_4 to A_1 as shown in Table 1. Large values of A_4 / A_1 cause a significant failure in surface energy balance closure.

2. Experimental Evaluation

To evaluate the theoretical analysis presented above, the data collected at the Amdo micrometeorological site (91° 37.5'E, 31° 14.5'N, 4800 m above m.s.l.) on 16 July 1998 during Global Energy and Water Cycle Experiment (GEWEX) Asian Monsoon Experiment (GAME) / Tibet are used here. The Amdo site was located in a flat prairie with sufficient fetch in all directions. The surface was almost bare soil in the pre-monsoon dry season, but was covered with scattered short grasses during the summer monsoon season (Tanaka et al., 2001). The soil at the site was of medium texture. Details on the instruments and various data processing techniques are provided at the Web site: http://monsoon.t.u-tokyo.ac.jp/tibet/data/iop/pbltower/doc/anduo.html. Fluxes of sensible heat (H) and latent heat (LE) were measured by eddy covariance using a sonic anemo-thermometer (DAT-300, Kaijo) and an infrared hygrometer (AH-300, Kaijo). A clinometer was also used to measure sensor inclination. The infrared hygrometer was used to detect the high frequency fluctuation. A capacity-type hygrometer and thermometer (Pt-100) were also set near the infrared hygrometer, and used to measure the low frequency fluctuation of the specific humidity. These instruments were mounted at 2.85 m above ground and about 20 m from the tower. Sampling rate was 10 Hz, and the raw data were collected for post data processing. Appropriate corrections were made for nonzero mean vertical velocity, flux loss owing to sensor separation (0.15 m) between sonic anemometer and hygrometer, and density variation owing to simultaneous transfer of H and LE [Webb et al., 1980].

Four components of radiation, upward and downward fluxes of short wave and long wave radiation, were measured and recorded by an independent system. The sensors used were EKO MS-801 (short wave radiation) and Eppley PIR (long wave radiation). In measuring the long wave radiation, the dome and the base temperatures of each radiometer were also measured for correction with secondary long wave emission from the domes of sensors (Shimura 1960). A data logger (VAISALA, QLC50) sampled the data every second and recorded the 10-minutes averages. In order to synchronize the logger clock with that of the tower system, the records of downward shortwave radiation from both systems were used. (Tanaka et al., 2001). The surface skin temperature was measured by an IR thermometer (Optex HR1-FL). Soil heat flux was measured with two heat transducers (EKO MF-81) buried 0.10 and 0.20 m below the ground surface. The heat storage above the transducers was calculated from the time variation of soil temperatures with their soil water contents.

Figure 4 shows (a) diurnal variations of surface radiation flux components, i.e., downward shortwave radiation (DSR), downward longwave radiation (DLR), upward shortwave radiation (USR), and upward longwave radiation (ULR) fluxes; (b) same as (a) but for net radiation (Rn), sensible heat (H), latent heat (LE), and soil heat (G_0) fluxes; and (c) surface effective radiative temperature ($Tsfc$) which is measured by using the IR thermometer during the daytime of 16 July 1998 at Amdo site of GAME/Tibet experiments. One good reason to use this day for a case study is that it is a sunny day which dramatically decreases the complexities caused by intermittent clouds.

DSR, USR, ULR, Rn, H, LE, G_0, and $Tsfc$ varied diurnally, DSR, USR, ULR, Rn, H, and LE had phases similar to $Tsfc$, and DSR, USR, ULR, Rn, H, LE, and $Tsfc$ reached their peaks at 14:30 (local time). G_0 reached its peak at 12:30 (local time) yielding $\delta = 2.0$ hours (or $2.0\pi/12$ in rad). The maximum value ($G_{0\max}$) of G_0 is 264.4 W m^{-2} and the maximum value of $Rn_{\max}$ is 694.5 Wm^{-2}.

$G_{0\max}/Rn_{\max} = 0.38$, which corresponds with A_4/A_1 between $2.2/6$ and 2.4/6 in Table 1. Figure 5 shows the comparison between turbulent heat fluxes ($H + LE$) and surface available energy ($Rn - G_0$) during the daytime of 16 July 1998 at the Amdo site of the GAME/Tibet experiments. The slope of the regression line forced to pass through the origin of the coordinates is 0.73. It is between $\varepsilon = 0.722$ and $\varepsilon = 0.76$ for A_4/A_1 between $2.2/6$ and 2.4/6 in Table 1. Figure 5b is similar to Figure 3b. The data (dot) collected before 14:30 when the Rn (or $Tsfc$) were distributed above the regression line and the others (circle)were distributed under the regression line.

3. Discussion

For most moist soil surfaces, the phase difference (δ) between soil surface heat flux and temperature ranges from 0 to $\pi/4$. However, in our equation derivation, we assumed that the surface boundary condition is sinusoidal as shown in Equation (3). Actually, the diurnal variation of soil surface temperature does not strictly follow symmetric sinusoids, e.g., Gao *et al*. (2007). For instance, in both morning and afternoon, the absolute values of soil surface temperature gradients in time are larger than that of the ideal sinusoid given in Figure 1. This should help alleviate the overestimation in surface energy balance ratio (ε) in the morning, and the underestimation in surface energy balance ratio (ε) in the afternoon. Previous observations (e.g., Figure 6 in Oncley *et al*., 2007) of surface energy components indicated a significant phase difference between soil surface heat flux (G_0) and turbulent heat fluxes (H and LE). This difference may negatively influence energy balance closure.

Our theoretical analysis builds on assumption that Rn, H, and LE have identical phases with soil surface temperature. Although this assumption is not strictly realistic in experiments, e.g., the phase of LE is not strictly identical with that of soil surface temperature at the Amdo site as shown in Figure 4, the fact that the phases Rn, H, and LE are close to that of the soil surface temperature support our present assumption and analysis.

The imbalance was prevalent not only on a half-hour basis, but also on a daily or an annual basis (Wilson et al. 2002). However, we used data from one sunny day (16 July, 1998) rather than data from several days or months data to validate our theoretical analysis, because (1) it is easier to see the phase difference between surface energy components and surface temperature on a representative sunny day, and intermittent clouds which often occur during this experimental period over the Tibetan plateau may negatively influence our energy analysis; and (2) energy balance closure at this site for the entire experimental period was analyzed by Tanaka (2001).

Actually, because the wind speed and direction keep changing at sites the source areas of surface energy components can not be strictly matched (Foken, 2008), and except for measurement errors and storage terms, long wave eddies or organized turbulence structures are also main reasons for the closure problems. The land surface energy balance closure has therefore been a challenging problem; and our current work just focuses on a narrow aspect of land surface energy balance closure.

4. Summary

The phase difference between soil surface heat flux and temperature was characterized and found to range from 0 to $\pi/4$ for natural soils, where the diurnal variation in soil temperature was assumed to be sinusoidal. The impact of phase difference between soil surface heat flux and temperature on surface energy closure was theoretically examined for both moist land and dry soil surfaces. A case study was used for experimental evaluation.

We concluded that the phase difference of soil surface heat flux from those of net radiation, sensible heat and latent heat fluxes was an inherent source to soil surface energy balance closure failure. We showed that $H + LE$ was always less than $Rn - G_0$ for ideal conditions when all energy components were accurately measured, their footprints were strictly matched, and all corrections were made. The energy balance closure ratio ε was extremely sensitive to the ratio of soil surface heat flux amplitude to net radiation flux amplitude, and a large value of A_4 / A_1 caused a significant failure in surface energy balance closure.

Acknowledgements

This study was supported by MOST (2006CB400600, 2006CB403500, and 200603805005), by CMA (GYHY(QX)2007-6-5), and by the Centurial Program sponsored by the Chinese Academy of Sciences. The work described in this publication was also supported by the European Commission (Call FP7-ENV-2007-1 Grant nr. 212921) as part of the CEOP – AEGIS project (http://www.ceop-aegis.org/) coordinated by the Université Louis Pasteur. This study was partly supported by the Hatch Act and State of Iowa funds. We appreciate Professor Ishikawa Hironhiko (from the Disaster Prevention Research Institute, Kyoto University, Kyoto, Japan) for kindly providing us the data collected at Amdo site during GAME/Tibet. We appreciate Professor Zhongbo Su (from Spatial Hydrology and Water Resources Management, Department of Water Resources, International Institute for Geo-Information Science and Earth Observation (ITC), the Netherlands) for his comments. We are very grateful to the anonymous reviewers for their careful review and valuable comments, which led to substantial

improvement of this manuscript.

References

Bruin H. A. R. de and Holtslag A. A. M.: A simple parameterization of the surface fluxes of sensible and latent heat during daytime compared with the Penman-Monteith concept, J. Appl. Meteorol., 21, 1610-1621, 1982.

Cava, D., Contini, D., Donateo, A., and Martano P.: Analysis of short-term closure of the surface energy balance above short vegetation, Agricultural and Forest Meteorology, 148: 82-93, 2008.

Chen, F., and Dudhia J.: Coupling an advanced land-surface/hydrology model with the Penn State-NCAR MM5 modeling system, part I, Model implementation and sensitivity, Mon. Weather Rev., 129, 569–582, 2001.

Elagina L. G, Kaprov B. M., and Timanovskii D. F.: A characteristic of the surface air layer above snow. Izv Acad Sci USSR, Atmos Ocean Phys 14:926–931 (in Russian), 1978.

Elagina L.G., Zubkovskii S. L., Kaprov B. M., and Sokolov D. Y.: Experimental investigations of the energy balance near the surface (in Russian). Trudy GGO 296:38–45, 1973.

Foken, T., Kukharets, V. P., Perepelkin, V. G., Tsvang, L. R., Richter, S. H., and Weisensee, U.: The influence of the variation of the surface temperature on the closure of the surface energy balance, in 13th Symposium on Boundary Layer and Turbulence, Dallas, TX., 10 15 Jan. 1999, Amer. Meteorol. Soc., pp. 308-309, 1999.

Foken, T., Wimmer, F., Mauder, M., Thomas, C., and Liebethal C.: Some aspects of the energy balance closure problem, Atmospheric Chemistry and Physics, 6:4395-4402, 2006.

Foken, T.: The energy balance closure problem: An overview. Ecological Applications, 18(6): 1351-1367, 2008.

Gao, Z. Bian L., Hu Y., Wang L., and Fan J.: Determination of soil temperature in an arid region, Journal of Arid Environments. 71 , 157-168 , dio: 10.1016/j.jaridenv.2007.03.012, 2007.

Gao, Z., Chae N., Kim J., Hong J., Choi T., Lee and H.: Modeling of surface energy partitioning, surface temperature, and soil wetness in the Tibetan prairie using the Simple Biosphere Model 2 (SiB2), J. Geophys. Res., 109, D06102, doi:10.1029/2003JD004089, 2001.

Gao. Z., Fan X., and Bian L.: An analytical solution to one-dimensional thermal conduction-convection in soil. Soil Science, 168(2): 99-107, 2003.

Horton, R., and Wierenga P. J.,: Estimating the soil heat flux from observations of soil temperature near the surface. Soil Sci. Soc. Am. J., 47: 14-20,1983.

Jacobs A. F. G., Heusinkveld B. G., and Holtslag A. A. M. : Towards Closing the Surface Energy Budget of a Mid-latitude Grassland, Boundary-Layer Meteorol., 126:125–136, DOI 10.1007/s10546-007-9209-2, 2007.

Kanemasu E.T., Verma S. B., Smith E. A., Fritschen L.Y., Wesely M., Fild R. T., Kustas W. P., Weaver H., Steawart Y. B., Geney R., Panin G. N., and Moncrieff J. B.: Surface flux measurements in FIFE: an overview. J Geophys Res 97:18,547–18,555, 1992

Ma, Y., Kang, S., Zhu, L., Xu, B., Tian, L., and Yao, T.: Tibetan Observation and Research Platform- Atmosphere–land interaction over a heterogeneous landscape, Bull. Amer. Meteor. Soc., 89, 1487–1492, 2008.

Ochsner, T. E., Sauer T. J., and Horton R.: Field tests of the soil heat flux plate method and some alternatives. Agron. J., 98:1005-1014, DIO:10.2134/agronj2005.0249, 2006.

Ochsner, T. E., Sauer T. J., and Horton R.: Soil heat storage measurements in energy balance studies. Agron. J., 99:311-319, DIO:10.2134/agronj2005.0103s,2007.

Oncley, S. P., Foken T., Vogt R., Kohsiek W., DeBruin H. A. R., Bernhofer C., Christen A., van Gorsel E., Grantz D., Feigenwinter C., Lehner I., Liebethal C., Liu H., Mauder M., Pitacco A., Ribeiro L., Weidinger T. : The energy balance experiment EBEX-2000. Part I: overview and energy balance, Boundary-Layer Meteorol. 123:1–28, DOI 10.1007/s10546-007-9161-1, 2007.

Sauer, T. J., Ochsner T. E., and Horton R.: Soil heat flux plate: Heat flow distortion and thermal contact resistance. Agron. J., 99:304-310, DIO:10.2134/agronj2005.0038s, 2007.

Sellers, P. J., Los S. O., Tucker C. J., Justice C. O., Dazlich D. A., Collatz G. J., and Randall D. A.: A revised land surface parameterization (SiB2) for atmospheric GCMs. part II: The generation of global fields of terrestrial biophysical parameters from satellite data, J. Clim., 9, 706– 737, 1996b.

Sellers, P. J., Randall D. A., Collatz G. J., Berry J. A., Field C. B., Dazlich D. A., Zhang C., Collelo G. D., and Bounoua L.: A revised land surface parameterization (SiB2) for atmospheric GCMs. part I: Model formulation, J. Clim., 9, 676–705, 1996a.

Su, Z., Timmermans, W., Gieske, A., Jia, L., Elbers, J. A., Olioso, A., Timmermans, J., Van Der Velde, R., Jin, X., Van Der Kwast, H., Nerry, F., Sabol, D., Sobrino, J. A., Moreno, J. and Bianchi, R.: Quantification of land-atmosphere exchanges of water, energy and carbon dioxide in space and time over the heterogeneous Barrax site, International Journal of Remote Sensing, 29:17, 5215- 5235, 2007.

Tanaka, K., Ishikawa, H, Hayashi, T., Tamagawa, I., and Ma, Y.: Surface energy budget at Amdo on the Tibetan Plateau using GAME/Tibet IOP98 data, Journal of Meteorological Society of Japan, 79(1B): 505-517, 2001.

Van Wijk, W.R. and De Vries, D.A.: Periodic temperature variations in a homogeneous soil. In: Physics of Plant Environment (ed. W.R. Van Wijk), pp. 103–143. North-Holland, Amsterdam, 1963.

Wilson, K., Goldstein, A., Falg, E., Aubinet, M., Baldocchi, D., Berbigier, P., Bernhofer, C., Ceulemans, R., Dolman, H., Field, C., Grelle, A., Ibrom, A., Law, B. E., Kowalski, A., Meyers, T., Moncrieff, J., Monson, R., Oechel, W., Tenhunen, J., Valentini, R., and Verma, S.: Energy balance closure at FLUXNET sites, Agricultural and Forest Meteorology, 113: 223-243, 2002.

Figure captions

Figure 1. Theoretical demonstration of temporal variations in soil surface temperature [$T(0,t)$], soil temperature [$T(z,t)$], soil surface heat flux [$G(0,t)$], soil heat flux [$G(z,t)$], and soil heat storage $C_g z\partial T/\partial t$ during daytime.

Figure 2. Theoretical demonstration of a) temporal variations in surface energy components (Rn, H, LE, and G_0) during daytime, and b) comparison between turbulent heat fluxes ($H+LE$) and surface available energy ($Rn-G_0$).

Figure 3. Same as Figure 2 but with a different distribution of G_0 and the curves and

dots are in blue for the afternoon.

Figure 4. (a) diurnal variations of surface radiation flux components, i.e., downward shortwave radiation (DSR), downward longwave radiation (DLR), upward shortwave radiation (USR), and upward longwave radiation (ULR) fluxes; (b) same as (a) but for net radiation (Rn), sensible heat (H), latent heat (LE), and soil heat (G_0) fluxes; and (c) surface effective radiative temperature ($Tsfc$) for daytime on 16 July 1998 at the Amdo site of the GAME/Tibet experiments.

Figure 5. Comparison between turbulent heat fluxes ($H + LE$) and surface available energy ($Rn - G_0$) for daytime on 16 July 1998 at the Amdo site of the GAME/Tibet experiments.

Table 1 Sensitivity of surface energy balance ratio $\varepsilon \equiv (H + LE)/(Rn - G_0)$ to the value of A_4 / A_1.

A_4 / A_1	ε
0.3/6	0.983
0.4/6	0.977
0.5/6	0.970
0.6/6	0.963
0.7/6	0.955
0.8/6	0.946
1.0/6	0.937
1.2/6	0.928
1.4/6	0.907
1.6/6	0.883
1.8/6	0.857
1.9/6	0.828
2.0/6	0.795
2.2/6	0.760
2.4/6	0.722
2.6/6	0.682
2.8/6	0.639
3.0/6	0.593

Fig.1

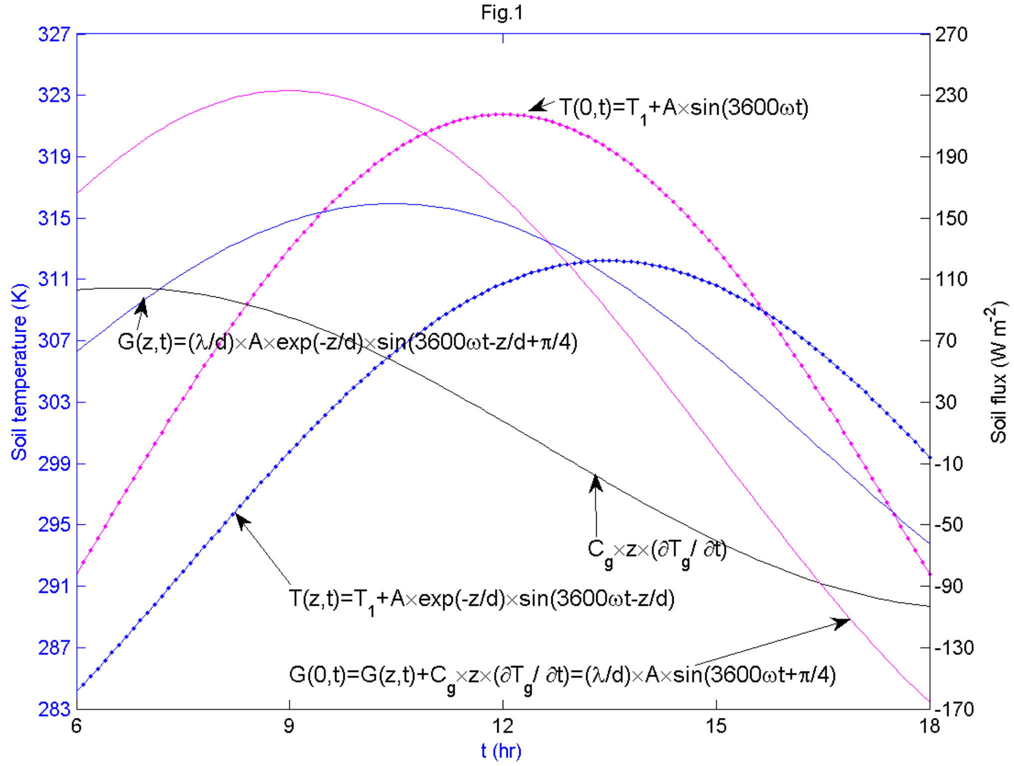

Soil temperature (K)
Soil flux (W m-2)
t (hr)
T(0,t)=T1+A×sin(3600ωt)
G(z,t)=(λ/d)×A×exp(-z/d)×sin(3600ωt-z/d+π/4)
Cg×z×(∂Tg/ ∂t)
T(z,t)=T1+A×exp(-z/d)×sin(3600ωt-z/d)
G(0,t)=G(z,t)+Cg×z×(∂Tg/ ∂t)=(λ/d)×A×sin(3600ωt+π/4)

Fig.2

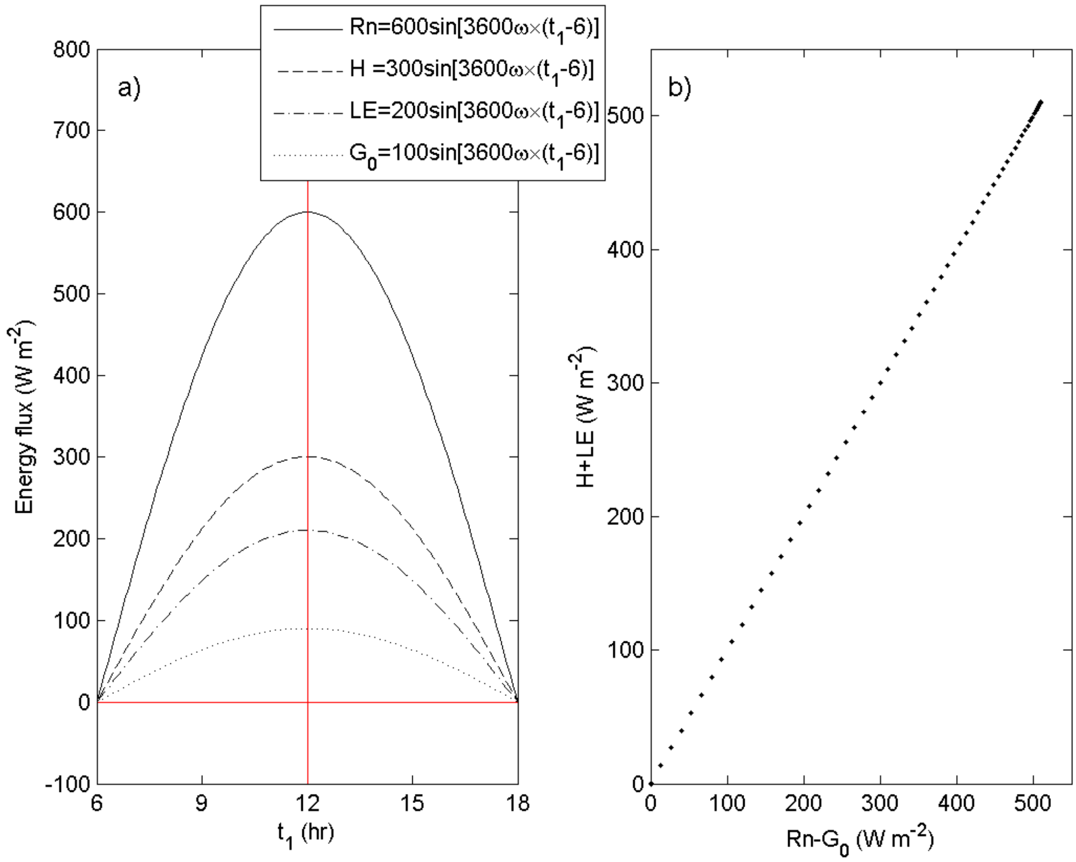

Rn=600sin[3600ω×(t1-6)]
H =300sin[3600ω×(t1-6)]
LE=200sin[3600ω×(t1-6)]
G0=100sin[3600ω×(t1-6)]
a)
Energy flux (W m-2)
t1 (hr)
b)
H+LE (W m-2)
Rn-G0 (W m-2)

Fig.3

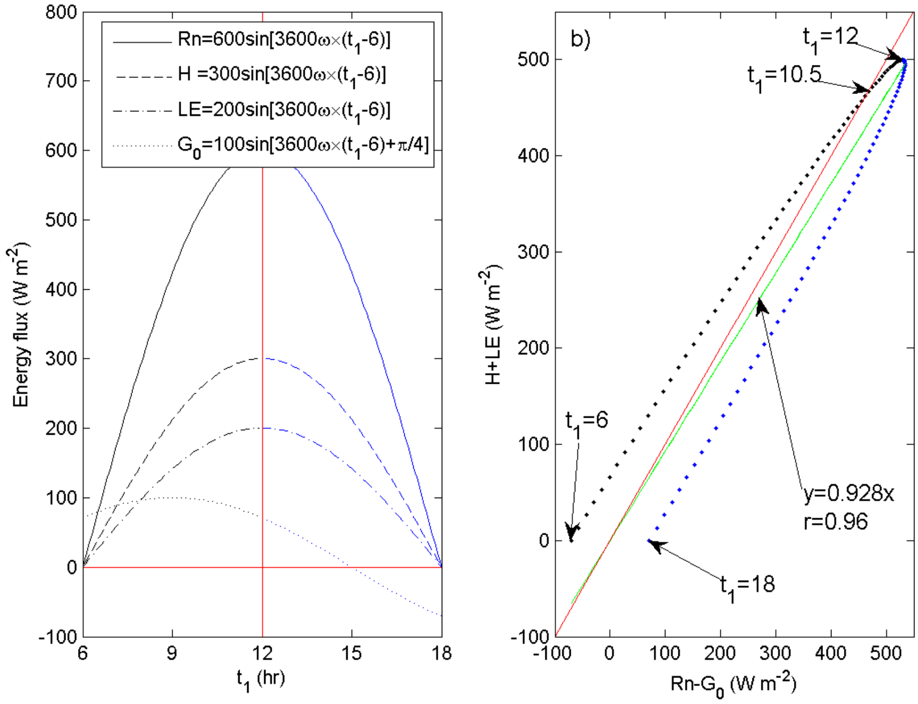

Rn=600sin[3600ω×(t1-6)]
H =300sin[3600ω×(t1-6)]
LE=200sin[3600ω×(t1-6)]
G0=100sin[3600ω×(t1-6)+π/4]
Energy flux (W m-2)
t1 (hr)
b)
t1=12
t1=10.5
t1=6
y=0.928x
r=0.96
t1=18
H+LE (W m-2)
Rn-G0 (W m-2)

1

2

Fig. 4

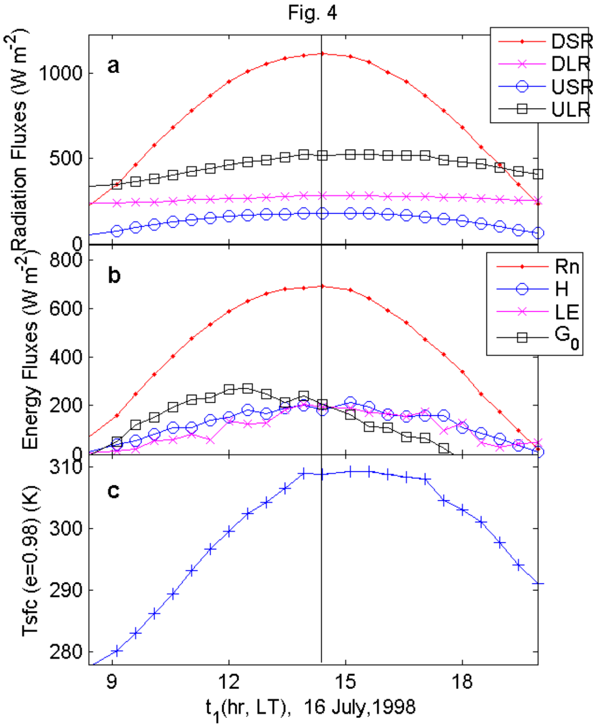

Radiation Fluxes (W m^{-2})
1000
500
0
a
DSR
DLR
USR
ULR
Energy Fluxes (W m^{-2})
800
600
400
200
0
b
Rn
H
LE
G$_0$
Tsfc (e=0.98) (K)
310
300
290
280
c
9
12
15
18
t$_1$(hr, LT), 16 July,1998

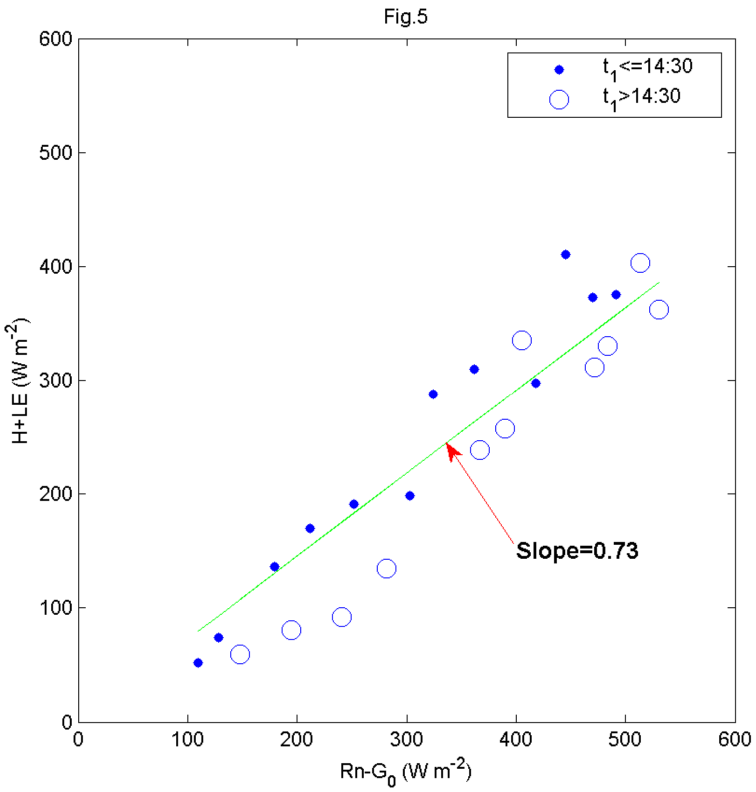
Fig.5
600
500
400
300
200
100
0
0
100
200
300
400
500
600
H+LE (W m-2)
Rn-G0 (W m-2)
t1<=14:30
t1>14:30
Slope=0.73